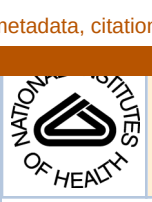

Application of the Aqueous Porous Pathway Model to Quantify the Effect of Sodium Lauryl Sulfate on Ultrasound-Induced Skin Structural Perturbation

Baris E. Polat, **Jennifer E. Seto**, **Daniel Blankschtein**[*], and **Robert Langer**
Department of Chemical Engineering, Massachusetts Institute of Technology, Cambridge, MA 02139, USA

Abstract

This study investigated the effect of sodium lauryl sulfate (SLS) on skin structural perturbation when utilized simultaneously with low-frequency sonophoresis (LFS). Pig full-thickness skin (FTS) and pig split-thickness skin (STS) treated with LFS/SLS and LFS were analyzed in the context of the aqueous porous pathway model to quantify skin perturbation through changes in skin pore radius and porosity-to-tortuosity ratio (ε/τ). In addition, skin treatment times required to attain specific levels of skin electrical resistivity were analyzed to draw conclusions about the effect of SLS on reproducibility and predictability of skin perturbation. We found that LFS/SLS-treated FTS, LFS/SLS-treated STS, and LFS-treated FTS exhibited similar skin perturbation. However, LFS-treated STS exhibited significantly higher skin perturbation, suggesting greater structural changes to the less robust STS induced by the purely physical enhancement mechanism of LFS. Evaluation of ε/τ values revealed that LFS/SLS-treated FTS and STS have similar transport pathways, while LFS-treated FTS and STS have lower ε/τ values. In addition, LFS/SLS treatment times were much shorter than LFS treatment times for both FTS and STS. Moreover, the simultaneous use of SLS and LFS not only results in synergistic enhancement, as reflected in the shorter skin treatment times, but also in more predictable and reproducible skin perturbation.

Keywords

Permeation Enhancers; Skin; Surfactants; Transdermal; Ultrasound

INTRODUCTION

Enhancement of skin permeability by the application of ultrasound is referred to as sonophoresis. Although the use of ultrasound for transdermal delivery of therapeutics dates back to the 1950s, extensive research in this area has only taken place in the past two decades.[1,2] In the early years of sonophoresis research, therapeutic frequencies, ranging from 1–3 MHz, were most common.[3–5] However, a significant shift in the methodology and understanding of sonophoresis took place once the switch was made to low-frequency sonophoresis (LFS, utilizing frequencies in the range of 20 – 100 kHz), because it was possible to achieve even greater skin permeability enhancements compared to therapeutic frequencies.[6] Following this shift, research on the mechanisms of LFS showed conclusively that cavitation above the skin, in the aqueous coupling medium, is the primary mechanism of enhancement.[7,8] Much of this initial mechanistic research involving LFS was done

[*]Corresponding author: Professor Daniel Blankschtein, Department of Chemical Engineering, Room 66-444, Massachusetts Institute of Technology, 77 Massachusetts Avenue, Cambridge, MA 02139, USA, Tel: +1 617 253 4594, Fax: +1 617 252 1651, dblank@mit.edu.

utilizing pure aqueous media, containing no chemical enhancers in the coupling solution.[6–9] However, another breakthrough in the field occurred when it was shown that combining LFS with a chemical enhancer, specifically a surfactant such as sodium lauryl sulfate (SLS), caused a synergistic effect, resulting in orders-of-magnitude improvements in skin permeability enhancement over the application of LFS alone.[10–14] Since that time, the synergistic effect between chemical enhancers (mainly SLS) and LFS has been well documented,[2,10–12,15] although the precise physical mechanisms responsible for the observed synergism are still not well understood. Nearly all previous studies on LFS/SLS synergism have focused primarily on the effect of a simultaneous SLS and LFS treatment in order to increase skin permeability to different solutes. Although the extent to which LFS/SLS enhances skin permeability, relative to LFS alone, is generally well understood, very little is known about how these synergistic enhancers affect the skin structure itself. To date, only a small number of publications have commented on the structural changes in skin treated with LFS/SLS and LFS.[16–18] These studies provided useful microscopy-based insight into the structural changes that occur when LFS/SLS and LFS are applied to skin. In the present study, the aqueous porous pathway model is implemented to probe changes in skin structural parameters and to draw quantitative conclusions about the role of SLS in inducing skin perturbation.

With the above in mind, it is clear that a quantitative study investigating the effect of LFS/SLS on skin structural parameters, compared to that of LFS alone, would provide significant insight on how adding SLS to the LFS coupling medium affects skin perturbation. Furthermore, because LFS/SLS combines both physical and chemical enhancement mechanisms, while LFS acts solely in a physical manner, it is likely that the mechanical properties of the skin model used may also play an important role in determining the extent of skin perturbation.[9,19,20] Specifically, pig full-thickness skin (FTS), which possesses a full dermal backing, may impart increased mechanical support to the skin in response to the physical perturbation induced by LFS, relative to pig split-thickness skin (STS, dermatomed to 700 μm thickness). In fact, Seto *et al.* have recently shown that when treating skin with LFS/SLS at 20 kHz, the thickness of the skin plays a significant role in determining the extent of skin perturbation in human skin models (250 μm STS, 700 μm STS, and FTS), while in pig skin models, skin thickness does not play a significant role (700 μm STS and FTS).[19] Moreover, the difference in LFS/SLS treatment times for pig and human 700 μm STS reported by Seto *et al.* led the authors to propose that intrinsic skin differences (e.g., dermal elastic fiber content) may explain the observed differences. In this manuscript, we utilize an approach similar to the one used by Seto *et al.* to gauge overall skin perturbation. Specifically, we utilize the aqueous porous pathway model to calculate two skin structural parameters: (i) log C, which is related to the average radius of the aqueous skin pores, and (ii) the porosity-to-tortuosity ratio (ε/τ). We compare the structural parameters of skin treated with LFS/SLS and LFS to that of untreated skin (for both FTS and STS), to better understand the effect of SLS on skin structural perturbation and transdermal pathways when utilized in combination with LFS. Furthermore, we also explore the reproducibility and predictability of the LFS/SLS and LFS treatments by comparing: (i) the width of the 95% confidence intervals for the structural parameters calculated, (ii) the correlation coefficient observed between the permeability and the resistivity of skin samples (see Theory section), and (iii) the trends observed in treatment times for skin samples treated to different extents of skin electrical resistivity. Clearly, the reproducibility and predictability of skin permeability enhancement are essential for the successful clinical implementation of this technology.[21,22]

With the above motivation and background in mind, it is important to stress that the study presented here is the first one to investigate the synergism between LFS and SLS in the context of quantifying skin structural perturbation, while utilizing a *fixed skin electrical*

resistivity protocol. It is noteworthy that previous studies have focused primarily on fixed treatment time protocols (typically treating skin samples with LFS for 10 minutes in the presence and in the absence of SLS).[11,12,15] The present study differs from previous ones in that we treated skin samples with both LFS/SLS and LFS to attain a wide range of skin electrical resistivity levels, allowing treatment times to vary in order to reach those levels. This modification in the treatment protocol is significant, because treating skin samples with LFS for a fixed period of time does not ensure that the skin samples are perturbed to any significant extent. Indeed, skin permeability enhancement is usually modest under this type of treatment protocol, since LFS application for 10 minutes results in just a 1.5-fold enhancement in skin electrical resistivity.[12] Note that this is a very small extent of skin electrical resistivity enhancement, considering that skin hydration itself can cause similar extents of enhancement during a 24-hour period.[12] Accordingly, in the present study, we require that LFS be applied to attain greater enhancements in skin electrical resistivity, which allows us to better understand the effect of the purely physical enhancement mechanism associated with LFS, relative to the combined physical and chemical enhancement mechanisms associated with LFS/SLS.

Along the lines discussed above, the objectives of the present study are to explain: i) how the extent of skin perturbation differs between skin samples treated with LFS/SLS and LFS, in the context of the aqueous porous pathway model, ii) how ε/τ ratios differ between skin samples treated with LFS/SLS and LFS, iii) how the amount of mechanical support (i.e., the thickness of the dermis in the skin model considered) affects the extent of skin perturbation in samples treated with LFS/SLS and LFS, and iv) how the reproducibility and predictability of skin permeability enhancement and treatment times of skin samples treated with LFS/SLS compares to those of skin samples treated solely with LFS. Addressing (i) – (iv) will help explain the role of SLS in inducing skin structural perturbation, including the role of SLS in enhancing transdermal transport.

MATERIALS AND METHODS

Chemicals

Phosphate buffered saline tablets (PBS; 0.01 M phosphate, 0.137 M NaCl) and SLS were obtained from Sigma Chemical Company (St. Louis, MO). C_{14}-labeled sucrose (specific activity of 600 mCi/mmol) was obtained from American Radiolabeled Chemicals (St. Louis, MO). Hionic-Fluor, a scintillation cocktail, was obtained from Perkin-Elmer (Waltham, MA). All chemicals were used as received. Deionized water from a Milli-Q water purification system (Millipore, Bedford, MA) was used for the preparation of all solutions.

Preparation and Pre-Treatment of Skin Samples by LFS/SLS

Previously published protocols were utilized for the storage and preparation of skin samples.[14,19] This procedure has been approved by the MIT Committee on Animal Care. Briefly, skin was harvested from the back and flank of Female Yorkshire pigs, sectioned into 25-mm strips, and stored at −85 °C for up to 6 months. Before use in experiments, the skin was thawed for 1 hour in PBS and all excess hair and subcutaneous fat were removed. Full-thickness skin (FTS) samples were utilized without further preparation, while split-thickness skin (STS) samples were dermatomed to 700 μm thickness using an electric reciprocating dermatome (Zimmer Orthopedic Surgical Products, Dover, OH). The skin was then cut into 25 mm by 25 mm samples, for use in the 15-mm inner diameter diffusion cells (PermeGear, Hellertown, PA).

LFS/SLS and LFS pre-treatment of skin samples was carried out according to previously published methods.[12,13,17,19,20,24] Skin treatment was carried out with a 20 kHz

ultrasound horn (VCX 500, Sonics and Materials, Inc., Newtown, CT), under the following experimental conditions: intensity - 7.5 W/cm^2, duty cycle - 50% (5 s on, 5 s off), and tip displacement - 3 mm. Two different coupling media were utilized to treat the skin samples: i) 1% SLS in PBS solution (LFS/SLS treatment), and ii) PBS solution alone (LFS treatment). Samples were treated with LFS until they reached currents ranging from 5 μA (low level of LFS treatment) to 200 μA (high level of LFS treatment), in order to test a wide range of LFS-induced skin perturbation (higher currents suggest higher levels of skin perturbation). Note that the range of skin currents used here is similar to previously reported ranges used with LFS.19,25 After each minute of LFS treatment, the coupling medium was changed in order to minimize thermal effects (maintain the temperature within 10 °C of room temperature), and the electrical current of the skin samples was measured to determine if a desirable skin current had been attained. Following LFS treatment, samples were rinsed thoroughly with PBS in order to remove all excess SLS from the skin surface, and the coupling medium was replaced with PBS prior to the sucrose permeability experiments.

Skin Electrical Resistivity Measurements

Skin electrical resistivity, *R*, has been shown to be an accurate and instantaneous indicator of the structural state of the skin.9,19,23 Previously published methods9,24,25 were followed to measure *R* and are summarized next. A signal generator (Hewlett-Packard, model HP 33120A) was used to generate an AC voltage at 100 mV and 10 Hz. The voltage was applied across the skin using two Ag/AgCl electrodes (In Vivo Metrics, Healdsburgh, CA). The skin electrical current was measured using a multimeter (Fluke Corporation, Model 189) and the skin electrical resistance was calculated using Ohm's Law. *R* was then calculated by subtracting the background resistance and then multiplying the resulting skin electrical resistance by the area of the skin sample. In order to ensure that the skin was intact prior to experimentation, the initial *R* value of a skin sample was required to be above 50 kOhm·cm^2.26–28

Calculating the Steady-State Sucrose Skin Permeability

Following the LFS/SLS or LFS treatments, the steady-state sucrose skin permeability was determined. Sucrose was chosen as a model hydrophilic permeant because it has previously been utilized in the context of the aqueous porous pathway model to accurately describe skin perturbation with LFS/SLS through the measurement of aqueous pore radii and the calculation of ε/τ values.19,20 Before commencing the permeability experiments, skin samples were remounted into clean, dry diffusion cells, and filled with 12 mL of PBS in the receiver chamber. For both the LFS/SLS-treated and the LFS-treated skin samples, 2 mL of donor solution containing 0.3–5 μCi/mL of C_{14}-labeled sucrose was utilized. For the passive skin samples, 0.75–1.0 mL of donor solution containing 25–50 μCi/mL of C_{14}-labeled sucrose was utilized (note that a higher concentration is necessary because of the low permeability of the untreated skin samples, and therefore, a smaller donor volume is utilized to minimize the amount of radiolabeled chemicals used). The radiolabeled sucrose concentrations were chosen such that the level of radioactivity in the receiver chamber aliquots was significantly greater than the background radioactivity levels (approximately 10-fold greater). The receiver chambers were stirred magnetically at 400 rpm.

The diffusion cells were sampled every two hours, between 18 and 26 hours, in order to measure the steady-state sucrose permeability of the skin samples. Note that this time frame has previously been established as being appropriate for measuring the steady-state permeability of sucrose through porcine skin.19,20 For skin samples treated with LFS/SLS or LFS, 200-μL aliquots of the donor solutions and 400-μL aliquots of the receiver solutions were withdrawn at each time point, in addition to measuring *R*. For passive skin samples, 20-μL aliquots of the donor solutions and 500-μL aliquots of the receiver solutions were

withdrawn at each time point. Upon withdrawal of solution from the receiver chamber, an identical volume of PBS was added in order to keep the solution level constant. The concentration of sucrose in each sample was measured by adding 5 – 15 mL of scintillation cocktail to each sample and then analyzing the samples on a Tri-Carb 2810TR liquid scintillation counter (PerkinElmer, Waltham, MA).

The permeability of sucrose through the skin, P, was calculated at steady-state, infinite sink conditions using the following equation:20

$$P=\frac{V}{AC_d}\left(\frac{\Delta C}{\Delta t}\right) \quad (1)$$

where A is the area of skin available for permeation, V is the volume of PBS in the receiver chamber, C_d is the average sucrose concentration in the donor chamber over the sampling period, and $(\Delta C/\Delta t)$ is the rate of change of sucrose concentration in the receiver chamber (where replacement of the sampled aliquots by PBS is taken into account).

THEORY

The Aqueous Porous Pathway Model

By assuming that a hydrophilic permeant, such as sucrose, follows a similar path through the skin as the current carrying ions (for PBS, the dominant ions are Na^+ and Cl^-), one can utilize the aqueous porous pathway model to calculate meaningful structural parameters of the skin.20 This model utilizes hindered-transport theory29 in order to quantify the steric hindrance exerted by the finite radius of the skin pores on the fluxes of the aqueous permeant and the current carrying ions through the skin. The hindrance factors corresponding to both species are related solely to the radius of each permeant and to the average radius of the aqueous skin pores, r_{pore}. Then, by equating the diffusion of the aqueous permeant, which is related to the skin permeability, P, and the diffusion of the current carrying ions, which is related to the skin electrical resistivity, R, one can determine a log C value (see Eq. (2) below), which is related to r_{pore} and the extent of skin structural perturbation.

The relation between skin permeability, P, and skin electrical resistivity, R, in the context of the aqueous porous pathway model, is given by:20

$$\log P=\log C-\log R \quad (2)$$

where C is defined as follows:

$$C=\frac{kT}{2z^2Fc_{ion}e_0}\cdot\frac{D_p^{\infty}H(\lambda_p)}{D_{ion}^{\infty}H(\lambda_{ion})} \quad (3)$$

where z is the electrolyte valence, F is Faraday's constant, c_{ion} is the electrolyte molar concentration, e_0 is the electronic charge, k is the Boltzmann constant, T is the absolute temperature, D_i^{∞} is the infinite-dilution diffusion coefficient of solute i, $H(\lambda_i)$ is the hindrance factor for solute i, and λ_i is defined as the ratio of the radius of solute i, r_i, to the radius of the aqueous skin pores, r_{pore}.13 The most up-to-date expression for $H(\lambda_i)$, which is valid for $\lambda_i \leq 0.95$, is given by:14,19,29

$$H(\lambda_i)=1+\frac{9}{8}\lambda_i \ln \lambda_i - 1.56034\lambda_i + 0.528155\lambda_i^2 + 1.91521\lambda_i^3 - 2.81903\lambda_i^4 + 0.270788\lambda_i^5 + 1.10115\lambda_i^6 - 0.435933\lambda_i^7 \quad (4)$$

It is important to note that the only variable in Eq. (3) that depends on the intrinsic properties of the skin is r_{pore} (which appears through λ_p and λ_{ion}). All the other variables are either constants or are properties of the permeants used. Therefore, once an experimental C value is determined using Eq. (2), r_{pore} can be determined by iteratively solving Eq. (3) until it converges.

Before applying the aqueous porous pathway model to an experimental data set, it is first necessary to determine whether the model is applicable. To this end, a linear regression is fit to each set of log P versus log R data sets, and only if a 95% confidence interval on the slope of the regression includes the theoretical value of −1 (see Eq. (2)) and the linear regression is found to be statistically significant, is the model assumed to be valid. For a more detailed discussion on the applicability of the aqueous porous pathway model, see Seto *et. al.*19 After confirming that the data set can be described by the aqueous porous pathway model, a log C value is determined using Eq. (2) for each data point contained within the data set. Subsequently, all the individual log C values are averaged to yield the log C value corresponding to that data set. The average log C value can then be utilized to calculate r_{pore} and to assess the structural perturbation of the skin.

It is important to stress that, for any aqueous permeant utilized (with given hydrodynamic radius), only a certain range of r_{pore} values can be determined. In fact, for any permeant, there will be an upper bound on the value of r_{pore} that can be probed depending on the hydrodynamic radius of the permeant (the hydrodynamic radius of sucrose is estimated to be 5.5 Å20). This follows, because as the pores become increasingly large, the amount of hindrance exerted by the pores on the diffusing permeants becomes increasingly small as the hindrance factor approaches unity. Recall that hindrance factors range from 0 to 1, where a hindrance factor of 1 corresponds to no hindrance, and a hindrance factor of 0 corresponds to infinite hindrance. Beyond a certain r_{pore} value, the hindrance exerted by the pores on the permeant becomes statistically indistinguishable from the diffusion of the permeant at infinite dilution, which corresponds to the upper bound of r_{pore} (calculated from the corresponding upper bound on log C) that can be probed with that permeant. This infinite-dilution limit (or infinite-pore limit) will be attained at lower r_{pore} values for smaller permeants and will be higher for larger permeants. The infinite-pore limit for sucrose has been previously established to be ~120 Å (based on Eq. (4)).19,20 Therefore, for pore radii which are larger than the upper bound for sucrose, log C values can still be used to compare relative skin perturbations of different skin samples.

In addition to calculating log C and r_{pore} values in the context of the aqueous porous pathway model, we can also use this model to compute the porosity-to-tortuosity ratio (ε/τ) of the skin samples. This allows us to gain deeper insight into the transdermal pathways present within the skin, by understanding the importance of the area of skin pores present on the skin surface (reflected in ε) relative to the length of the aqueous pathways present in the skin (reflected in τ). Specifically, ε/τ is given by the following expression:20

$$\left(\frac{\varepsilon}{\tau}\right)=\frac{1}{\left(\frac{R}{\Delta x}\right)\sigma_{sol}H(\lambda_{ion})} \quad (5)$$

where σ_{sol} is the electrical conductivity of PBS (0.012 Ω^{-1}`cm^{-1}),20 $H(\lambda_{ion})$ is the hindrance factor for an ion calculated using Eq. (4), and Δx is the thickness of the skin layer that provides the primary barrier to transport, which is assumed to be the thickness of the stratum corneum (13.1 μm).13,30

RESULTS

Analysis of the Experimental Data in the Context of the Aqueous Porous Pathway Model

In order to verify that the aqueous porous pathway model is valid over the range of *R* values attained using the LFS/SLS and LFS skin treatments, we determined if the regressed slopes are not significantly different from the theoretical value of −1 (see Eq. (2)). The log *P*-log *R* plots generated for this analysis are reported in Figure 1, with the resulting linear regression parameters listed in Table I. Note that a subset of the LFS/SLS data has been published in 19. Table I shows that the 95% confidence intervals on the slopes of all 6 sample sets tested include the theoretical value of −1, thus validating use of the model.* After establishing the applicability of the aqueous porous pathway model, we proceed next to calculate skin structural parameters to assess the effect of SLS on skin perturbation, when utilized simultaneously with LFS.

Evaluation of Skin Perturbation through a Comparison of Log *C* Values

To assess the overall skin perturbation of the two LFS/SLS-treated and two LFS-treated skin models, an analysis-of-variance (ANOVA) test was performed on all the log *C* values corresponding to the four sample groups tested (see Table II). The ANOVA test yielded $P<0.0001$ (note that, at 95% confidence, *P* must be below 0.05 to reject the null hypothesis that all the sample groups tested have the same population mean), indicating that one or more of the four sample groups do not contain the same population mean. Additional analysis showed that there is no statistical difference in the log *C* values of the two LFS/SLS-treated skin models (FTS and STS), while there is significant statistical difference between FTS and STS treated solely with LFS ($P<0.0001$). Next, an ANOVA test was performed on the LFS/SLS-treated FTS and STS models, along with the LFS-treated FTS model, and no statistical difference in the log *C* values of these three skin models was observed. Pairwise t-tests assuming unequal variances between the log C values of all the four skin models confirmed that the LFS-treated STS model exhibits a significantly different extent of skin perturbation compared to the other three skin models tested, while none of the other three skin models tested are statistically different from each other.

As a reference point, log *C* values for untreated FTS and STS were also determined, and the two LFS/SLS-treated and two LFS-treated skin models were found to have significantly different log *C* values than the untreated skin samples (pairwise t-tests at 95% confidence). Furthermore, a comparison of untreated FTS and untreated STS showed no statistical difference in their log *C* values. Utilizing Eqs. (3) and (4), the average aqueous pore radius of untreated FTS was found to be 16.4 Å (95% confidence interval of [13.6 Å, 21.8 Å]), and that of STS was found to be 16.6 Å (95% confidence interval of [14.2 Å, 20.5 Å]). Note that for the LFS/SLS-treated and LFS-treated skin samples, the calculated pore radii were above the infinite-pore limit (see Theory section) and, therefore, only log *C* values were used to compare the extent of skin structural perturbation of these skin models.

*Note that for the passive skin samples (samples with no LFS/SLS or LFS treatments), there is greater uncertainty in the slope of the data, as reflected in the large range for the 95% confidence intervals for these two data sets (1.48 and 0.87, respectively). This is expected, because the passive skin samples have very similar electrical resistivities due to the inherent barrier properties of the skin, and because we require that the skin samples have a certain initial electrical resistivity to ensure their integrity. Therefore, any natural variation in skin permeability, or in skin pore radius distribution, will result in relatively large deviations from expected values and cause greater uncertainty in the regressed values.

Evaluation of the Skin Structural Parameter, ε/τ

ε/τ values were calculated using Eq. (5) for the two LFS/SLS-treated and two LFS-treated skin samples, as well as for untreated FTS and STS. These results are reported in Table II. The ε/τ values of both LFS/SLS-treated FTS and STS are identical, while the ε/τ values of the LFS-treated FTS and STS groups are lower, and generally decrease with decreasing skin thickness. There is no statistical difference between the ε/τ values of untreated FTS and STS. On average, ε/τ was found to increase approximately 20-fold between untreated skin samples and samples that were treated with LFS/SLS or LFS, suggesting an increase in the number of pores on the skin (reflected in a larger ε value) or the creation of more direct (less tortuous) paths through the skin (reflected in a smaller τ value) following treatment of the skin.

Treatment Time Required to Reach Specific Skin Electrical Resistivity Levels

In order to assess reproducibility and predictability of the LFS/SLS and LFS treatment regimens, in addition to the regression analyses (r^2 values and 95% confidence intervals) reported in Tables I and II, treatment times were compared for each of the two treatment conditions (with and without SLS) at three separate skin perturbation levels (as quantified by R values of 1.5, 4.0, and 10.0 kΩ·cm^2±40%). Note that a smaller skin electrical resistivity value corresponds to a greater extent of skin perturbation (less resistance of the skin membrane). This data is reported in Table III. For LFS/SLS-treated skin samples, treatment times increased monotonically with decreasing skin electrical resistivity. In addition, treatment times were not significantly different between FTS and STS samples at each of the skin electrical resistivities considered. On the other hand, the treatment times for skin samples treated solely with LFS did not behave in a straightforward manner, and took 5-fold to 12-fold longer to reach skin electrical resistivity levels similar to those of skin samples treated with LFS/SLS. In addition, no statistically significant difference was found between the treatment times required to reach any of the three skin electrical resistivities considered in the case of LFS-treated FTS.

DISCUSSION

Effect of SLS on the Structural Perturbation of LFS-Treated Skin

The primary criterion that we used to quantify skin perturbation utilizes the effective radii of the hydrophilic diffusive pathways in the skin models tested, which scale directly with log C in the context of the aqueous porous pathway model (see Eqs. (2) – (4)). A less negative log C value indicates an increase in the pore radius, suggesting increased perturbation of the skin samples by the treatment administered. Our main objective was to compare the results for skin samples treated with LFS/SLS with those for skin samples treated only with LFS, in order to understand the effect of SLS on skin perturbation when used simultaneously with LFS. In addition, in order to test the effect of the skin mechanical support on skin perturbation, for the two skin treatments used (LFS/SLS and LFS), both FTS (typical thickness of 1.5–1.8 mm) and STS (thickness of 0.70 mm) models were tested. It is important to recognize that both the FTS and STS models are equivalent, in the context of the aqueous porous pathway model, prior to treatment, as clearly reflected in their: (i) nearly identical log C values (see Table II, corresponding to pore radii of 16.4 Å and 16.6 Å, respectively), and (ii) their statistically similar values of ε/τ (see Table II). Therefore, any observed increases in log C or ε/τ in the treated skin samples can be attributed solely to the LFS/SLS or LFS treatments applied to those skin samples.

Comparison of the LFS/SLS-Treated FTS and STS Models—A comparison of the skin structural parameters of LFS/SLS-treated FTS and STS shows that: (i) their log C values are statistically similar (see Table II), and (ii) their ε/τ values are essentially identical

(see Table II). Furthermore, Table III shows that the treatment times associated with the three levels of skin electrical resistivity for FTS and STS are statistically similar for the three skin electrical resistivities analyzed. This confirms that, irrespective of the skin thicknesses studied, skin perturbation induced by LFS/SLS is generated in a consistent and similar manner. In other words, the FTS and STS models are identical in terms of their response to the LFS/SLS treatment. This important conclusion is consistent with the recent findings by Seto *et al.*19

Comparison of log C Values for LFS/SLS-Treated and LFS-Treated Samples— For LFS-treated FTS, the extent of skin perturbation, as quantified by the log *C* values, is statistically similar to both LFS/SLS-treated FTS and LFS/SLS-treated STS. However, as Table II shows, the log *C* value corresponding to LFS-treated STS is significantly lower than those corresponding to the other three skin sample groups tested (pair-wise t-tests comparing LFS-treated STS to the other three sample groups yields $P \leq 0.006$). This interesting finding follows because: i) in the absence of SLS, skin samples must be treated for much longer time periods to reach similar skin electrical resistivity values (see Table III), and ii) the thinner STS model does not respond to the physical enhancement mechanism (cavitation) associated with LFS in the same manner as the thicker FTS model. Simply stated, the stresses put on the thinner, less mechanically robust STS during the long LFS treatment induces significantly greater skin perturbation than that observed in: (i) the more mechanically robust FTS model, and (ii) the combined chemical/physical enhancement induced by the shorter LFS/SLS treatment. This finding also shows that, although the skin electrical resistivity is a good quantitative measure of skin perturbation, the extent to which it scales with skin permeability depends on both the skin model and skin treatment regimen used.

Comparison of ε/τ Values for LFS/SLS-Treated and LFS-Treated Samples— Table II shows that the ε/τ values for the LFS-treated samples decrease with decreasing skin thickness, and are generally lower than those corresponding to the LFS/SLS-treated samples. Although the observed differences are not statistically significant to 95% confidence, they are nevertheless interesting because they provide some insight into the role that SLS plays in perturbing the skin, when combined with LFS. More specifically, although the LFS/SLS-treated samples are subjected to 5- to 12-fold shorter treatments (see Table III), these samples still have higher ε/τ values, suggesting that they are either more porous (larger ε value) and/or less tortuous (smaller τ value) than those treated only with LFS. It is not likely that an increase in ε can explain the difference in ε/τ values for LFS/SLS-treated and LFS-treated skin samples. This is because previous studies have shown that the radius of impinging cavitation microjets and the overall number of cavitation events observed near the skin surface decreases in LFS/SLS-treated samples, with respect to samples treated solely with LFS.11,12 Since cavitation bubble collapse near the skin surface is the primary mechanism of new pore formation and permeability enhancement for skin treated with LFS/SLS and LFS, this would in fact suggest that the porosity of LFS-treated samples should be greater than the porosity of LFS/SLS-treated samples (which is further enhanced because LFS treatments are an order-of-magnitude longer than LFS/SLS treatments). Therefore, the most likely explanation for the observed increase in ε/τ in LFS/SLS-treated samples, with respect to LFS-treated samples, is the ability of SLS to fluidize/disorder lipid bilayers and expand lacunar regions, thereby creating less tortuous and more direct permeation pathways through the skin membrane. Note that this explanation is consistent with the findings of Paliwal *et al.*, who showed that, in LFS-treated skin, the number density of lacunar regions increases significantly with respect to those in untreated and LFS/SLS-treated skin (which suggests greater porosity).18 In addition, Paliwal *et al.* showed that in LFS/SLS-treated skin, the number density of lacunar regions did not increase with respect to that in untreated skin, although the total area of the lacunar regions did increase. This suggests increased length

and connectivity of the lacunar regions, which could be explained by an interconnected three-dimensional network of pores (which suggests decreased tortuosity).18 Accordingly, the ability of LFS and SLS to work in concert, in order to permeabilize skin in both a physical and chemical manner, leads to the observed higher ε/τ values for the LFS/SLS-treated samples, compared to the samples treated only with LFS.

Reproducibility and Predictability of Skin Perturbation in Samples Treated with LFS/SLS and LFS

Reproducibility and predictability of skin perturbation are important characteristics of any skin treatment regimen. Clinically, not all patients have skin with similar thickness, elasticity, or other biomechanical properties.31,32 Therefore, a robust skin treatment protocol is ideal. Consequently, examining the data presented in this paper, it is not surprising that a combination of LFS/SLS is presently used in clinical applications of LFS (the company commercializing this technology is Echo Therapeutics, Franklin, MA).21,22

An examination of the log *P*-log *R* plots shown in Figure 1 reveals much greater variability in the regression lines shown for samples treated solely with LFS (Figures 1(c) and 1(d)), compared to those treated with LFS/SLS (Figures 1(a) and 1(b)). This is also shown quantitatively in Tables I and II, where the 95% confidence intervals for both the slope of the linear regression and the log *C* values are broader for the LFS-treated samples (0.33–0.37 and 0.10–0.13, respectively) compared to those for the LFS/SLS-treated samples (0.09–0.22 and 0.05–0.09, respectively). Similarly, the r^2 values for the linear regressions of the LFS-treated data (0.53–0.57) are smaller than those of the LFS/SLS-treated data (0.73–0.92), thus demonstrating that skin perturbation, and the resulting skin permeability enhancement, are less predictable for skin treated solely with LFS.

Another significant difference between the LFS/SLS-treated and LFS-treated samples is in the observed trends in treatment times (see Table III). Specifically, samples treated with LFS/SLS take nearly an order-of-magnitude less time to reach similar skin electrical resistivities than LFS-treated samples do. Note that the observed decrease in treatment time is consistent with the previous finding that the energy density threshold required to observe skin permeability enhancement in LFS/SLS-treated skin is an order-of-magnitude smaller than that for LFS-treated skin (note that energy density scales with treatment time).11 In addition, LFS/SLS-treated samples behave in a more predictable manner, where: (i) treatment times decrease with increasing skin electrical resistivity, and (ii) the treatment times necessary to reach the various skin electrical resistivity levels considered are not significantly different for the FTS and STS samples. On the other hand, for FTS samples treated solely with LFS, treatment times show no statistically significant difference to reach the three skin electrical resistivity levels reported in Table III (an ANOVA analysis yielded a p-value of 0.172, which was confirmed by pairwise t-tests at 95% confidence), while the treatment times for LFS-treated STS samples decrease in a non-linear manner with increasing skin electrical resistivity levels. In addition, a comparison of treatment times for the LFS-treated FTS and STS samples reveals that, at the 1.5 $k\Omega\cdot cm^2$ skin electrical resistivity level, the treatment times are statistically similar, while they are statistically significantly different (95% confidence) at both the 4 and 10 $k\Omega\cdot cm^2$ levels. This again points to the lack of predictability and reproducibility of skin samples treated only with LFS, where some skin samples respond much more favorably to the LFS treatment than others. With all of the above in mind, it is quite clear that it is extremely advantageous to treat skin with a combination of LFS/SLS. Not only are the required treatments much shorter using LFS/SLS, but also the combined chemical and physical enhancement mechanisms involved in skin perturbation using LFS/SLS induce much more predictable trends in skin perturbation than those induced by the purely physical mechanism associated with LFS.

The most significant implications of our findings involve an improved mechanistic understanding of the combined effect of LFS and SLS on skin perturbation. Specifically, we have shown that, although not intuitive, the combination of both a chemical and physical skin penetration enhancer can, in fact, be less perturbing to the skin than a physical skin penetration enhancer alone. Furthermore, our results show that the addition of SLS to the LFS coupling medium not only allows the delivery of permeants in an equivalent manner to LFS alone, but also induces less perturbation to the skin membrane in a much shorter, reproducible, and predictable manner. Clearly, the reduction in treatment time in the presence of SLS is a great advantage clinically, because it would require health personnel an order of magnitude more time to treat patients with LFS alone. Furthermore, the importance of decreased skin perturbation and shorter application time is very significant with respect to patient safety and compliance. Future research in this area should be aimed at identifying surfactants that can provide similar, or greater, levels of skin permeability enhancement when combined with LFS, than LFS/SLS, while inducing even less skin perturbation and irritation. To this end, *in vivo* studies on the irritancy potential of the LFS/surfactant treatment of skin should be considered.

CONCLUSIONS

We investigated the effect of SLS on skin perturbation, when utilized simultaneously with LFS, by treating two skin models, pig FTS and pig STS, with two treatment regimens, LFS/SLS and LFS, to reach a range of skin electrical resistivity levels. The LFS/SLS treatment was found to provide consistent extents of skin perturbation, as quantified using the log *C* and ε/τ values obtained. Skin samples treated solely with LFS yielded less consistent results, where the log *C* values of the FTS and STS skin models were statistically significantly different. Additionally, the ε/τ values for LFS-treated skin samples were generally less than those for LFS/SLS-treated samples, suggesting that SLS acting on the skin creates more direct paths through the skin membrane by the disordering/fluidization of lipid bilayers, denaturation of keratin fibers, and expansion of lacunar regions. An analysis of the variability in the log *P*-log *R* linear regression parameters and log *C* values revealed greater variation in samples treated solely with LFS, resulting in lower r^2 values and broader confidence intervals for the regression parameters and log *C* values, with respect to LFS/SLS-treated samples. Additionally, the LFS-treated samples required 5-fold to 12-fold longer treatment times than the LFS/SLS-treated samples to reach similar skin electrical resistivity levels. Treatment times for the LFS/SLS-treated samples behaved predictably, decreasing monotonically with increasing skin electrical resistivity level, showing no significant difference in treatment times between FTS and STS samples at each of the skin electrical resistivity levels analyzed. On the other hand, LFS-treated samples were perturbed in a less predictable manner, with large variations and no statistical significance in treatment times between the skin electrical resistivity levels considered.

In summary, SLS has a generally positive impact on skin structural perturbation when utilized in combination with LFS, compared to LFS treatment alone, by: (i) requiring equal, or less, skin perturbation to reach similar skin electrical resistivity values (as reflected in the log *C* values), (ii) reaching similar skin electrical resistivity levels in much shorter treatment times (about an order-of-magnitude decrease in treatment times), and (iii) inducing skin perturbation in a significantly more reproducible and predictable manner.

Acknowledgments

We thank Professor Renata F.V. Lopez for her useful feedback during the preparation of this manuscript. This research was funded by the National Institutes of Health (Grant# EB-00351) and the U.S. Army Research Office through the Institute for Solider Nanotechnologies at MIT (Grant# DAAD-19-02-D-002). JES was also supported

by a NSF Graduate Research Fellowship. The contents of this manuscript represent solely the views of the authors and do not necessarily reflect the position of the U.S. Government. No official endorsement should be inferred.

REFERENCES

1. Mitragotri S. Transdermal drug delivery using low-frequency sonophoresis. BioMEMS and Biomedical Nanotechnology. 2006:223–236.
2. Mitragotri S, Kost J. Low-frequency sonophoresis: a review. Adv Drug Deliv Rev. 2004; 56(5): 589–601. [PubMed: 15019748]
3. Johnson ME, Mitragotri S, Patel A, Blankschtein D, Langer R. Synergistic effects of chemical enhancers and therapeutic ultrasound on transdermal drug delivery. J Pharm Sci. 1996; 85(7):670–679. [PubMed: 8818988]
4. Levy D, Kost J, Meshulam Y, Langer R. Effect of ultrasound on transdermal drug delivery to rats and guinea pigs. J Clin Invest. 1989; 83(6):2074. [PubMed: 2498396]
5. Mitragotri S, Blankschtein D, Langer R. Ultrasound-mediated transdermal protein delivery. Science. 1995; 269(5225):850–853. [PubMed: 7638603]
6. Mitragotri S, Blankschtein D, Langer R. Transdermal drug delivery using low-frequency sonophoresis. Pharm Res. 1996; 13(3):411–420. [PubMed: 8692734]
7. Tang H, Wang CC, Blankschtein D, Langer R. An investigation of the role of cavitation in low-frequency ultrasound-mediated transdermal drug transport. Pharm Res. 2002; 19(8):1160–1169. [PubMed: 12240942]
8. Tezel A, Sens A, Mitragotri S. Investigations of the role of cavitation in low-frequency sonophoresis using acoustic spectroscopy. J Pharm Sci. 2002; 91(2):444–453. [PubMed: 11835204]
9. Tang H, Blankschtein D, Langer R. Effects of low-frequency ultrasound on the transdermal permeation of mannitol: comparative studies with in vivo and in vitro skin. J Pharm Sci. 2002; 91(8):1776–1794. [PubMed: 12115805]
10. Mitragotri S. Synergistic effect of enhancers for transdermal drug delivery. Pharm Res. 2000; 17(11):1354–1359. [PubMed: 11205727]
11. Mitragotri S, Ray D, Farrell J, Tang H, Yu B, Kost J, Blankschtein D, Langer R. Synergistic effect of low-frequency ultrasound and sodium lauryl sulfate on transdermal transport. J Pharm Sci. 2000; 89(7):892–900. [PubMed: 10861590]
12. Tezel A, Sens A, Tuchscherer J, Mitragotri S. Synergistic effect of low-frequency ultrasound and surfactants on skin permeability. J Pharm Sci. 2002; 91(1):91–100. [PubMed: 11782900]
13. Kushner J, Blankschtein D, Langer R. Experimental demonstration of the existence of highly permeable localized transport regions in low-frequency sonophoresis. J Pharm Sci. 2004; 93(11): 2733–2745. [PubMed: 15389675]
14. Polat B, Figueroa P, Blankschtein D, Langer R. Transport Pathways and Enhancement Mechanisms Within Localized and Non-Localized Transport Regions in Skin Treated with Low-Frequency Sonophoresis and Sodium Lauryl Sulfate. J Pharm Sci. doi 10.1002/jps.22280.
15. Lavon I, Grossman N, Kost J. The nature of ultrasound-SLS synergism during enhanced transdermal transport. Journal of Controlled Release. 2005; 107(3):484–494. [PubMed: 16165244]
16. Dahlan A, Alpar H, Stickings P, Sesardic D, Murdan S. Transcutaneous immunisation assisted by low-frequency ultrasound. International Journal of Pharmaceutics. 2009; 368(1–2):123–128. [PubMed: 19013510]
17. Kushner J, Kim D, So PT, Blankschtein D, Langer RS. Dual-channel two-photon microscopy study of transdermal transport in skin treated with low-frequency ultrasound and a chemical enhancer. J Invest Dermatol. 2007; 127(12):2832–2846. [PubMed: 17554365]
18. Paliwal S, Menon GK, Mitragotri S. Low-frequency sonophoresis: ultrastructural basis for stratum corneum permeability assessed using quantum dots. J Invest Dermatol. 2006; 126(5):1095–1101. [PubMed: 16528354]
19. Seto JE, Polat BE, Lopez RFV, Blankschtein D, Langer R. Effects of ultrasound and sodium lauryl sulfate on the transdermal delivery of hydrophilic permeants: Comparative in vitro studies with full-thickness and split-thickness pig and human skin. J Control Release. 2010; 145(1):26–32. [PubMed: 20346994]

20. Tang H, Mitragotri S, Blankschtein D, Langer R. Theoretical description of transdermal transport of hydrophilic permeants: application to low-frequency sonophoresis. J Pharm Sci. 2001; 90(5): 545–568. [PubMed: 11288100]
21. Becker B, Helfrich S, Baker E, Lovgren K, Minugh P, Machan J. Ultrasound with topical anesthetic rapidly decreases pain of intravenous cannulation. Acad Emerg Med. 2005; 12(4):289–295. [PubMed: 15805318]
22. Farinha A, Kellogg S, Dickinson K, Davison T. Skin impedance reduction for electrophysiology measurements using ultrasonic skin permeation: initial report and comparison to current methods. Biomed Instrum Techn. 2006; 40(1)
23. Karande P, Jain A, Mitragotri S. Relationships between skin's electrical impedance and permeability in the presence of chemical enhancers. J Control Release. 2006; 110(2):307–313. [PubMed: 16313994]
24. Kushner J, Blankschtein D, Langer R. Evaluation of hydrophilic permeant transport parameters in the localized and non-localized transport regions of skin treated simultaneously with low-frequency ultrasound and sodium lauryl sulfate. J Pharm Sci. 2008; 97(2):906–918. [PubMed: 17887123]
25. Kushner J, Blankschtein D, Langer R. Evaluation of the porosity, the tortuosity, and the hindrance factor for the transdermal delivery of hydrophilic permeants in the context of the aqueous pore pathway hypothesis using dual-radiolabeled permeability experiments. J Pharm Sci. 2007; 96(12): 3263–3282. [PubMed: 17887176]
26. Kasting GB, Bowman LA. Dc Electrical-Properties of Frozen, Excised Human Skin. Pharm Res. 1990; 7(2):134–143. [PubMed: 2308893]
27. Kasting GB, Bowman LA. Electrical Analysis of Fresh, Excised Human Skin - a Comparison with Frozen Skin. Pharm Res. 1990; 7(11):1141–1146. [PubMed: 2293212]
28. Rosell J, Colominas J, Riu P, Pallasareny R, Webster JG. Skin Impedance from 1 Hz to 1 Mhz. IEEE T Bio-Med Eng. 1988; 35(8):649–651.
29. Dechadilok P, Deen WM. Hindrance factors for diffusion and convection in pores. Ind Eng Chem Res. 2006; 45(21):6953–6959.
30. Johnson ME, Blankschtein D, Langer R. Evaluation of solute permeation through the stratum corneum: Lateral bilayer diffusion as the primary transport mechanism. J Pharm Sci. 1997; 86(10): 1162–1172. [PubMed: 9344175]
31. Cua A, Wilhelm K, Maibach H. Elastic properties of human skin: relation to age, sex, and anatomical region. Arch Dermatol Res. 1990; 282(5):283–288. [PubMed: 2221979]
32. Edwards C, Marks R. Evaluation of biomechanical properties of human skin. Clin Dermatol. 1995; 13(4):375–380. [PubMed: 8665446]

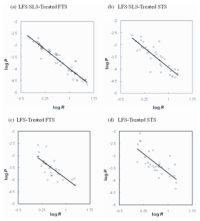

Figure 1.
Log *P*-log *R* plots for LFS/SLS-treated and LFS-treated skin samples. The solid line on each plot corresponds to the linear regression fitted to each data set. The regression parameters are listed in Table I.

Table I

Model validation for the skin treatments and skin thicknesses tested.

Treatment	Thickness	n	Linear Regression Parameters	
			Slope[a]	r^2
LFS/SLS	FTS	58	−1.08 ± 0.09	0.92
LFS/SLS	STS	37	−1.07 ± 0.22	0.73
LFS	FTS	30	−0.98 ± 0.33	0.57
LFS	STS	30	−1.02 ± 0.37	0.53
None	FTS	8	−1.01 ± 1.48	0.32
None	STS	11	−1.80 ± 0.87	0.71

[a] Range corresponds to a 95% confidence interval.

Table II

Structural parameter values for FTS and STS samples treated with LFS/SLS and LFS.

Treatment	Thickness	n	log $C^{a,b}$	$\varepsilon/\tau \cdot 10^{6}$ [a]
LFS/SLS	FTS	58	−2.96 ± 0.05	45.6 ± 12.7
LFS/SLS	STS	37	−2.90 ± 0.09	45.6 ± 13.3
LFS	FTS	30	−2.96 ± 0.10	42.0 ± 9.06
LFS	STS	30	−2.68 ± 0.13	36.1 ± 10.9
None	FTS	8	−3.35 ± 0.15	2.07 ± 0.50
None	STS	11	−3.34 ± 0.11	2.81 ± 0.40

[a] Range corresponds to a 95% confidence interval.

[b] log C is equivalent to the y-intercept of a linear regression of log P vs. log R with a slope equal to −1.

Table III

Skin treatment times associated with three levels of skin electrical resistivity,[a] for FTS and STS models treated with LFS/SLS and LFS.

		1.5 ± 0.6 kΩ·cm^2		4.0 ± 1.6 kΩ·cm^2		10.0 ± 4.0 kΩ·cm^2	
Treatment	**Thickness**	**n**	**time (min)[b]**	**n**	**time (min)[b]**	**n**	**time (min)[b]**
LFS/SLS	FTS	15	2.4 ± 0.4	11	2.0 ± 0.9	12	1.4 ± 0.6
LFS/SLS	STS	11	2.8 ± 1.2	10	1.8 ± 0.8	9	1.2 ± 0.4
LFS	FTS	10	14.0 ± 3.9	14	22.1 ± 5.3	4	16.5 ± 5.7
LFS	STS	8	13.1 ± 4.1	14	12.2 ± 4.7	6	6.4 ± 3.3

[a] These three ranges of *R* values were chosen in order to make useful statistical comparisons between the treatment times.

[b] Range corresponds to a 95% confidence interval.